JOURNAL OF VIROLOGY, Oct. 1994, p. 6243–6253
0022-538X/94/$04.00+0

Vol. 68, No. 10

Peripheral Blood Mononuclear Phagocytes Mediate Dissemination of Murine Cytomegalovirus

CHERYL A. STODDART,† RHONDA D. CARDIN, JESSICA M. BONAME, WILLIAM C. MANNING,‡ GERARDO B. ABENES, AND EDWARD S. MOCARSKI*

Department of Microbiology and Immunology, Stanford University School of Medicine, Stanford, California 94305-5402

Received 14 February 1994/Accepted 25 June 1994

Cytomegalovirus is transmitted with blood and organs from seropositive individuals, although the particular leukocyte population harboring latent or persistent virus remains poorly characterized. Murine cytomegalovirus, tagged with the *Escherichia coli lacZ* gene, was used to identify cells in which virus replicates during acute infection of immunocompetent mice. Recombinant murine cytomegaloviruses, RM461, RM460, and RM427, were constructed to express β-galactosidase under control of the human cytomegalovirus *ie1/ie2* promoter/enhancer. The *lacZ* gene was inserted between the *ie2* and *sgg1* genes in RM461 and RM460, disrupting a 0.85-kb late transcript that was found to be dispensable for replication in cultured cells as well as for infection of mice. In BALB/c mice, *lacZ*-tagged and wild-type viruses exhibited a similar 50% lethal dose and all had the capacity to latently infect the spleen. Peripheral blood mononuclear phagocytes were the major infected leukocyte cell type, as demonstrated by the ability of infected cells to adhere to glass and to phagocytize latex beads; however, these cells did not exhibit typical monocyte markers. Plaque assay for virus and 5-bromo-4-chloro-3-indolyl-β-D-galactopyranoside (X-Gal) staining of frozen sections of organs from infected mice revealed that the major target organs included the spleen, adrenal glands, liver, and salivary glands, although tissues as diverse as brown fat and lungs were also involved. Individual blue-staining cells were readily identified in all infected tissues. These studies identified a mononuclear phagocyte, possibly a macrophage or dendritic cell precursor, as the vehicle of virus dissemination during acute infection, and demonstrate the utility of using *lacZ*-tagged murine cytomegalovirus for tropism, pathogenesis, and latency studies.

Human cytomegalovirus (CMV) is a significant viral pathogen of immunocompromised adults and developing fetuses (1). The pathogenesis, tissue tropism, and latency characteristics of this virus are still poorly understood. Strict species specificity has limited the use of animal models (45), and therefore much of our current knowledge derives from studies of symptomatic CMV infection of immunocompromised individuals in whom cell-associated viremia involves polymorphonuclear, mononuclear, and endothelial cells (7, 12, 46, 51, 64). Much less is known about the interaction of human CMV with immunocompetent individuals. Blood leukocytes may be a source of virus spread in blood transfusion from healthy CMV-seropositive carriers (66), but whether a viremia ensues during primary infection remains unknown. Monocytes have been best documented as sites of persistence of human CMV DNA (61, 62); however, the role of these cells or other blood cell types in viral dissemination or persistence in the normal host has not been fully evaluated.

The difficulty of studying human CMV directly in humans has led to the use of murine, guinea pig, and rat CMV models. Investigations with murine CMV have reinforced biological similarities to human CMV and furthered an understanding of the tissue tropism (35, 54), pathogenesis (49, 52, 55), latency (25, 38), and immunology (15, 26, 31, 48, 53) of this group of viruses. Intraperitoneal (i.p.) inoculation of susceptible strains of mice, such as outbred Swiss-Webster or inbred BALB/c mice, leads to dissemination, with viral lesions in mouse spleen, liver, adrenal glands, and brown fat (36, 42, 43), which are all generally cleared of virus by an aggressive $CD8^+$ T-cell-mediated immune response beginning at 7 to 10 days postinoculation (p.i.) (15, 26). Sustained, high-level growth in salivary glands continues for over 1 month (35), and clearance of virus from this organ may be mediated by helper $CD4^+$ T cells and cytokines (20, 31).

Dissemination of murine CMV from sites of initial replication in the peritoneal cavity to various organs occurs via the blood. Virus associates with leukocytes during acute infection (2, 35) and is transmissible by blood transfusion during latent or persistent infection (6). Although peripheral blood mononuclear cells have been suspected of playing a crucial role in dissemination and macrophages support viral replication in the peritoneal cavity (3, 21, 41, 63), the blood cell type responsible for dissemination remains poorly characterized. Because of the importance of the spleen as a site for studying viral latency, spleen cells infected with murine CMV have been investigated by in situ hybridization-antibody colocalization methods (38). These studies have suggested that endothelial or sinusoidal lining cells act as the primary sites of replication in the spleen, extending earlier observations in which polyclonal antisera were used to localize murine CMV during acute infection (42). The salivary gland represents the site of sustained high-level replication of murine CMV, and infection in this gland is localized largely to serous acinar epithelial cells (36, 43).

Over the years, many different methods that have been used to identify virus-infected cells, ranging from the occurrence of characteristic cytopathology to the more sensitive and specific

* Corresponding author. Mailing address: Department of Microbiology and Immunology, Stanford University School of Medicine, Stanford, CA 94305-5402. Phone: (415) 723-6435. Fax: (415) 723-9180. Electronic mail address: mk.esm@forsythe.stanford.edu.

† Present address: Shaman Pharmaceuticals, Inc., South San Francisco, CA 94080.

‡ Present address: Department of Pediatrics, Stanford University School of Medicine, Stanford, CA 94305.

methods of immunofluorescence and in situ hybridization. Histological preservation of tissue integrity is highly variable and limits the use of these conventional approaches to identify rare infected cells present in the blood or organs. The localization of herpes simplex virus in tissues during acute and latent infection has been facilitated by the use of *lacZ*-tagged recombinant viruses whose presence can be readily detected in tissues by convenient and sensitive in situ staining methods (13, 14). By using *lacZ*-tagged murine CMV, we have achieved a highly sensitive means of detecting the presence of viruses with excellent preservation of tissue integrity and have identified the monocyte as a site of viral replication in the peripheral blood of immunocompetent BALB/c mice.

(A preliminary report of this work was presented at the 16th International Herpesvirus Workshop, Asilomar Conference Center, Pacific Grove, Calif., in 1991.)

MATERIALS AND METHODS

Viruses and cell culture. The Smith-K181 strain of murine CMV (obtained from M. Colin Jordan) was originally obtained as a salivary gland-passaged stock and, following plaque purification three times in our laboratory and evaluation for growth and virulence for BALB/c mice, was designated K181$^+$. Parental K181$^+$ and recombinant viruses were grown and plaque assayed in NIH 3T3 cells (ATCC CRL1658) in Dulbecco's modified Eagle's medium (Gibco-Life Technologies, Bethesda, Md.) supplemented with 10% NuSerum (Collaborative Research Inc., Waltham, Mass.), 100 U of penicillin per ml, 100 mg of streptomycin sulfate per ml, 0.66 mM arginine, 1.48 mM glutamine, and 0.24 mM asparagine. Prior to infection or transfection, cells were seeded into 6- or 12-well cell culture dishes (Falcon, Becton Dickinson) containing the same medium. Infections for the preparation of virus stocks and viral DNA were performed at a multiplicity of infection (MOI) of 0.0001 PFU per cell, and infections for the preparation of viral RNA were performed at an MOI of 10 PFU per cell. Tissue culture-propagated virus stocks were made by sonicating infected cells in a mixture of 50% medium and 50% autoclaved skim milk (35). Submaxillary salivary gland-propagated virus stocks were harvested 14 days after i.p. inoculation of 10^4 PFU of salivary gland-propagated RM461 and, after sonication, were stored as either a 10% or 25% (wt/vol) suspension in medium-skim milk. The inoculum for mock-infected control mice was prepared in a similar manner from uninfected salivary gland tissue. All virus stocks were stored at −80°C.

Animals, virus inoculation, and in situ staining. Three-week-old male BALB/c ByJ mice (Jackson Laboratories, Bar Harbor, Maine) were weight-matched prior to use between 24 and 28 days of age. Four-week old male SCID (C.B17 *scid/scid*) mice were bred locally at Stanford University School of Medicine, and nude (BALB/c *nu/nu*) were bred and used at the University of Western Australia. All animals received water and food ad libitum, were inoculated i.p. with either 10^6 PFU of tissue culture-propagated virus or 10^4 to 10^5 PFU of salivary gland-propagated virus, and were sacrificed by CO_2 asphyxiation, and organs were harvested for virus titer determinations as described previously (35), except that the lower limit of virus detection in this report was 10 PFU. Organs taken for cryosection were snap-frozen in polypropylene tubes containing OCT freezing medium (Miles, Indianapolis, Ind.) in a dry ice-ethanol bath and stored at −80°C. Sections (5 to 12 μm thick) were cut on a Bright Instrument cryostat, fixed in 0.5% glutaraldehyde, and stained with 300 μg of 5-bromo-4-chloro-3-indolyl-β-D-galactopyranoside (X-Gal) per ml to detect β-galactosidase (β-gal)-positive cells as described previously (13). In some cases, organs were fixed in 4% paraformaldehyde, stained overnight with X-Gal, embedded in paraffin, and sectioned (this was performed at the Diagnostic Pathology Laboratory, Stanford Medical Center). Rabbit polyclonal anti-human von Willebrand factor (Dakopatts, Glostup, Denmark) was used in indirect-immunofluorescence assays on acetone-fixed cells or tissue sections with rhodamine-conjugated goat anti-rabbit immunoglobulin G F(ab')$_2$ fragments (Tago, Burlingame, Calif.). The 50% lethal dose (LD_{50}) was determined as previously described (35).

For isolation of peripheral blood leukocytes, heart blood was collected into phosphate-buffered saline (PBS)–8 mM EDTA and erythrocytes were lysed by the addition of 150 mM ammonium chloride, after which cells were washed twice in cold PBS and suspended at 10^6 cells per ml. Leukocytes were either prepared by cytocentrifugation (Shandon Southern, Sewickley, Pa.) or allowed to incubate at 37°C on eight-well Labtek chamber slides (Miles Scientific, Elkhart, Ind.). Exposure of adherent cells to 5×10^6 3-μm-diameter latex beads (Polysciences, Warrington, Pa.) for 4 h was done as previously described (60). Slides were rinsed in PBS, fixed with 0.5% glutaraldehyde, and stained with X-Gal (13) or fixed with methanol and stained with May-Grünwald-Giemsa.

Recombinant plasmid and virus construction. pON432 carried a *Hpa*I-*Eco*RI fragment isolated from the right end of the *Eco*RI E fragment (pON400), which was cloned from the murine CMV genome (35) into pMT11 (56). A 3.9-kbp *Xho*I-*Bam*HI fragment from pON283 (5), consisting of the human CMV *ie1/ie2* promoter-enhancer (−219 to −19 relative to the transcription start site) fused to the *lacZ* gene and a simian virus 40 early polyadenylation signal (56), was inserted in either of two orientations into the unique *Hin*dIII site in pON432, after the fragment ends were filled in with Klenow DNA polymerase, thus generating pON460 and pON461. pON460 places the human CMV enhancer on the side closest to the murine CMV *ie2* gene, and pON461 places the human CMV enhancer on the side closest to the *sgg1* gene (Fig. 1). A *Hin*dIII site was reconstituted at the site upstream of the enhancer in each clone. Recombinant viruses RM460 and RM461 were constructed by cotransfection of *Pst*I-linearized pON460 or pON461 and intact murine CMV DNA into NIH 3T3 cells approximately 24 h after seeding at 50% cell density by using previously described methods (35). Before purification of individual recombinant viruses, the pool of virus from the cotransfection was used to inoculate mice i.p., and salivary gland-passaged virus stocks were prepared after 14 days. This step was included to subject candidate recombinants to the selective pressure of replicating in normal mouse tissues, to encourage the isolation of viruses capable of replicating in salivary glands, and to limit the number of recombinant viruses carrying adventitious mutations. *lacZ*$^+$ recombinants were isolated from this stock by triple plaque purification of blue-staining plaques on NIH 3T3 cells after X-Gal overlay (34, 57). For RM460 and RM461, five and seven plaque-purified recombinants, respectively, were isolated and examined by *Hin*dIII enzyme digestion, and all but one isolate in each set appeared to carry the insertion without any adventitious deletions elsewhere in the viral genome. Isolates with no unexpected alterations and with growth and latency characteristics of wild-type virus were chosen, and these were denoted RM460 and RM461, respectively (Fig. 1). The construction of RM427, a viral recombinant that carries mutations in the *ie2* and *sgg1* genes as well as a *lacZ* insertion under control of the same human CMV *ie1/ie2* promoter-enhancer fragment as RM460 and RM461, has been described previously (35).

RNA, DNA, and β-gal analyses. Protocols for isolation of

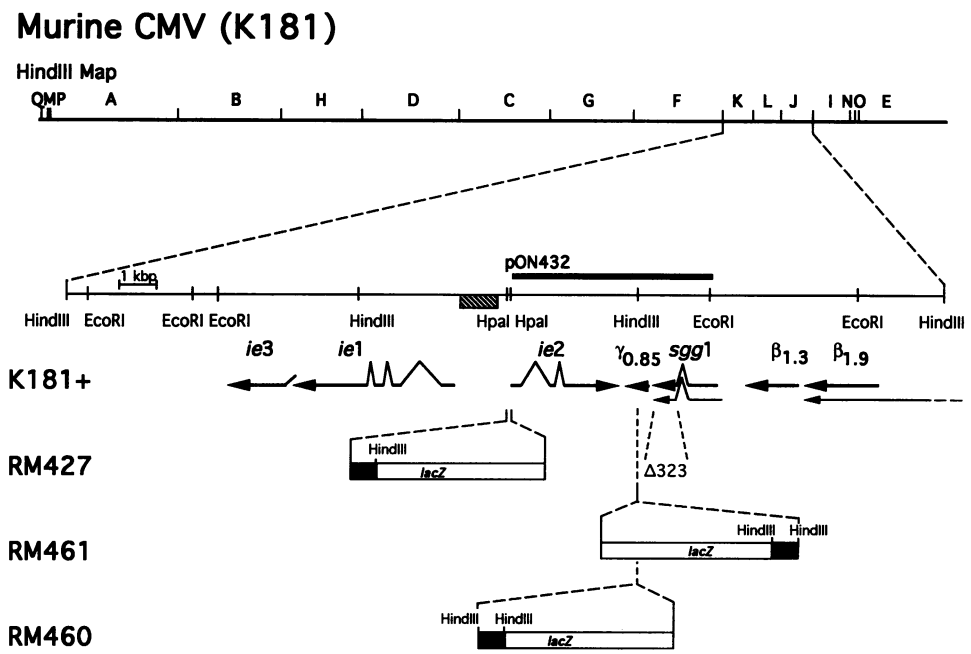

FIG. 1. Map position of mutations in RM427, RM461, and RM460. The *Hin*dIII map of the murine CMV (K181$^+$ strain) genome is shown on the top line. The *Hin*dIII J, K, and L fragments have been expanded to show the region containing the major α (immediate-early) *ie*1, *ie*2, and *ie*3 genes (23, 24, 39, 40), the *sgg*1 gene (35), and additional genes in the *Hin*dIII J region (65). The hatched box depicts the *ie*1/*ie*2/*ie*3 enhancer. The recombinant viruses are depicted in the lower portion. RM427, RM461, and RM460 each carry an insertion of *lacZ* under control of the human CMV *ie*1/*ie*2 promoter-enhancer. In RM427 the insertion replaces a 79-bp fragment between two *Hpa*I sites in the *ie*2 promoter, and this virus carries a spontaneous 323-bp deletion in the *sgg*1 gene (35). In RM461 and RM460, the insertion is in the depicted orientation within the *Hin*dIII L/J site. The positions of *Hin*dIII sites within and flanking each insertion are indicated.

RNA (10) and DNA (35), for treating cells with cycloheximide (34) or phosphonoformate (30), and for RNA blot hybridization (30) have all been published. The *ie*2-specific probe was a 0.9-kbp *Eco*RV-*Nhe*I fragment from pON401 (35), the *sgg*1-specific probe was an *Hin*dIII-*Eco*RI fragment from pON446 (35), the γ0.85-specific probe was a 0.26-kbp *Sph*I-*Dra*III fragment from pON467 located between the 3′ end of the *ie*2 gene and the *Hin*dIII L/J site (4), and the *lacZ*-specific probes were either a 1.16-kbp *Hpa*I fragment from pON405 (34) or a 3.5-kbp *Hin*dIII-*Eco*RI fragment from pON1 (56). Probes were isolated from an agarose gel and then radiolabeled with [α-^{32}P]dCTP (Amersham, Arlington Heights, Ill.) by the random-primed method as described previously (9). β-Gal levels were measured by replacing normal growth medium with medium supplemented with 4-methylumbelliferyl-β-D-galactoside (MUG) at a concentration of 150 mg/ml. This substrate freely diffuses into cells and is cleaved by β-gal, and the accumulated cleavage product diffuses into the medium and is detected at hourly intervals by a fluorometric assay as described previously (11). β-Gal activity was expressed as fold activation by calculating the ratio of MUG fluorescence level in replicate wells after infection with *lacZ*-tagged recombinant virus divided by the fluorescence after infection with parental K181$^+$ performed in parallel.

Latent infections and explant reactivation. Mice were inoculated i.p. with 10^6 PFU of tissue culture-propagated virus, and after 4 months, the animals were sacrificed by CO_2 asphyxiation. The spleen and salivary glands were removed from each animal. Salivary glands were sonicated and plated onto NIH 3T3 cell monolayers to detect actively replicating virus. The spleen was divided into three sections, and each was minced and plated with medium in three wells of a six-well multiwell dish. Virus was detected in the supernatant of the explant cultures by plaque assay on monolayer cultures of NIH 3T3 cells at weekly intervals through 6 weeks postexplant. Under these conditions, virus is only occasionally (1 in 15 animals) detected persistently replicating in the spleen. Consistent with the establishment of latency, explanted spleens did not yield detectable virus in the supernatant at 7 days but did so only after 14 days or longer in culture. Thus, animals used in these studies adhered to the operational criterion established for latent infection (59). At 4 months p.i., spleen explant culture (21) yielded virus reactivation in 90 to 100% of animals, and this level was observed whether tissue culture-propagated virus (10^6 PFU inoculated i.p.) or salivary gland-propagated virus (10^5 PFU inoculated i.p.) was used as inoculum.

RESULTS

Construction and characterization of RM460 and RM461. The two genes known to flank the *Hin*dIII site between the L and J fragments of the CMV genome, *ie*2 and *sgg*1, have each been found to be completely dispensable for growth in cultured fibroblast cells (34, 35). RNA blot hybridization had not detected any α or β transcripts other than *ie*2 and *sgg*1 in this region, and neither of these transcripts crossed this *Hin*dIII site (33, 35, 40). We therefore assessed the use of this *Hin*dIII site for the insertion of a *lacZ* marker gene to construct a virus that would be free of intentional disruptions of known viral genes. A chimeric *lacZ* gene under transcriptional control of the human CMV *ie*1/*ie*2 promoter-enhancer that had been previously incorporated into RM427 (35) was inserted in both orientations at this site. The resulting viruses, RM460 and RM461, were isolated from pools of candidates that had been subjected to passage through mice and isolated as a salivary gland stock collected 14 days after i.p. inoculation. This step

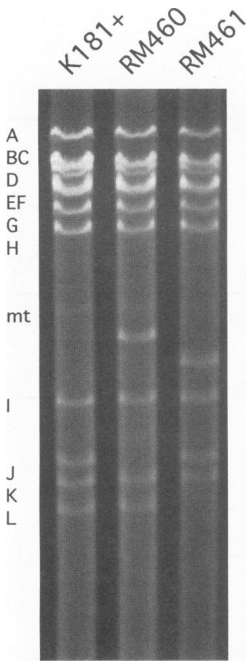

FIG. 2. *Hin*dIII restriction profiles of RM460 and RM461 compared with parental K181$^+$ DNA. Ethidium bromide-stained fragments after separation on a 0.5% agarose gel are depicted and labeled with the fragment name (37) to the left of the set of lanes. mt indicates the position of contaminating mitochondrial DNA in all lanes.

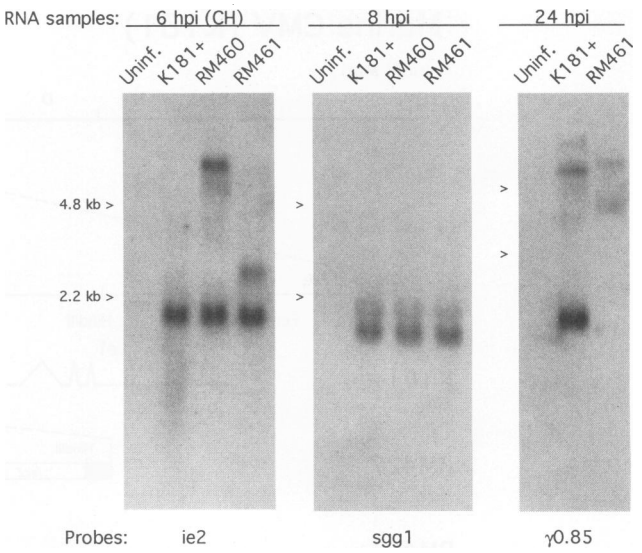

FIG. 3. RNA blot hybridization analysis of RM460 and RM461 transcripts. The source of the RNA is shown at the top and the probe is indicated at the bottom of each set of lanes. The probes are described in detail in Materials and Methods. Panels: 6 hpi (CH), whole-cell RNA accumulating in cells infected from 1 h before to 6 h after inoculation in the presence of 50 μg of cycloheximide (CH) per ml; 8 hpi, whole-cell RNA isolated at 8 h p.i.; 24 hpi, whole-cell RNA isolated at 24 h p.i. rRNA marker sizes are indicated to the left of the lanes.

was intended to encourage the isolation of recombinant viruses that retained full capability for growth and dissemination in the mouse host. The DNA fragment profile following *Hin*dIII digestion for both viruses, shown in Fig. 2, demonstrates that RM460 DNA had a new *Hin*dIII fragment of 12 kbp in place of the natural *Hin*dIII J fragment and RM461 had a new 11-kbp fragment replacing the natural *Hin*dIII L fragment. Each of these larger fragments was generated as predicted from the distribution of *Hin*dIII sites flanking the *lacZ* insert in the plasmids (Fig. 1). Comparison of *Hin*dIII and other restriction fragment profiles with those of parental virus showed that these viruses were free of deletions or insertions in any other region of the viral genome.

Gene expression by RM460, RM461, and RM427. Our initial concern was whether expression of the genes flanking the insert in RM460 and RM461 (*sgg*1 and *ie*2) had been altered (Fig. 3) by the insertion of the marker gene. Using an *sgg*1-specific probe on RNA collected 8 h p.i., we detected both the prominent 1.5-kb and less abundant 1.8-kb *sgg*1 transcripts in all viruses (Fig. 3). Thus, the two recombinant viruses exhibited the same pattern and level of expression of this β gene as the parental virus.

Using an *ie*2-specific probe to detect RNA that accumulated in the presence of a cycloheximide block, we detected the normal 1.75-kb *ie*2 transcript in RM460 and RM461 as well as novel transcripts through the *ie*2 region (Fig. 3). In RM460, the additional minor transcript was approximately 7.2 kb in size and was found to hybridize with a *lacZ* probe (data not shown). Therefore, this atypical transcript apparently arose as a result of transcription from the *ie*2 gene into the adjacent *lacZ* insert. In RM461, the minor 2.7-kb transcript failed to hybridize with either *lacZ* or *sgg*1 probes and thus probably represented a partially spliced form of the *ie*2 transcript not normally observed in parental K181-infected cells under cycloheximide block. Importantly, these unexpected transcripts were observed only in RNA made during cycloheximide treatment and were not observed when viral infection was allowed to proceed normally in the absence of drug block.

In the course of characterizing mRNAs in this region of the viral genome, a 0.85-kb γ transcript was detected and mapped to a position spanning the *Hin*dIII site (65). This γ0.85 transcript was found to be disrupted by the *lacZ* insertion in both RM461 (Fig. 3) and RM460 (data not shown).

We initially chose the human CMV *ie*1/*ie*2 promoter-enhancer fragment for insertion into the murine CMV genome because it was expected to direct high levels of expression of the marker gene. RM427, which carries the human CMV promoter-enhancer insert adjacent to the murine CMV enhancer, had been previously found to strongly express *lacZ* as an α gene when examined by RNA blot analysis (33). In contrast to our expectation, expression of the 3.6-kb *lacZ* transcript in either RM460 or RM461 was barely detectable at 6 h p.i. in the presence of cycloheximide or at 2 h p.i. in the absence of drug (data not shown). Rather, expression of the transcript and protein increased gradually throughout infection. Increasing levels of *lacZ* expression throughout infection were best revealed by incubating infected cells with MUG-containing medium at various times p.i. to measure the accumulation of β-Gal in cells (Fig. 4). We found that the accumulation of β-gal was blocked when phosphonoformate was present during infection, indicating that expression of the inserted *lacZ* gene exhibited kinetics more like a β or γ gene than an α gene (44). Thus, the human CMV promoter-enhancer-*lacZ* insert did not exhibit characteristics of an α gene when inserted at this site in the viral genome, and this seemed to correlate with both a failure to be active when protein synthesis was blocked and a failure to be shut off as normally occurs with murine CMV α gene expression (39, 47). As described above, cycloheximide treatment of RM460 in-

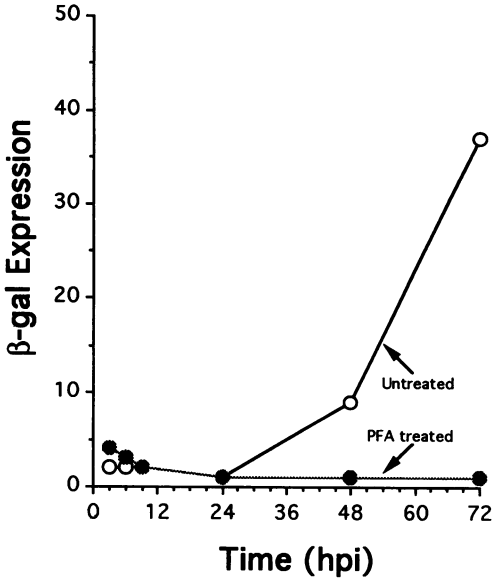

FIG. 4. High-level β-gal production by RM461 requires viral DNA replication. NIH 3T3 cells infected with an MOI of 1 PFU per cell were incubated for 1 h with MUG-containing medium at the indicated times, and fluorescence was measured and expressed as relative units. Phosphonoformate (PFA, 100 μg/ml) was added to one set of cultures (shaded circles) at the time of inoculation and was maintained during incubation with MUG-containing medium.

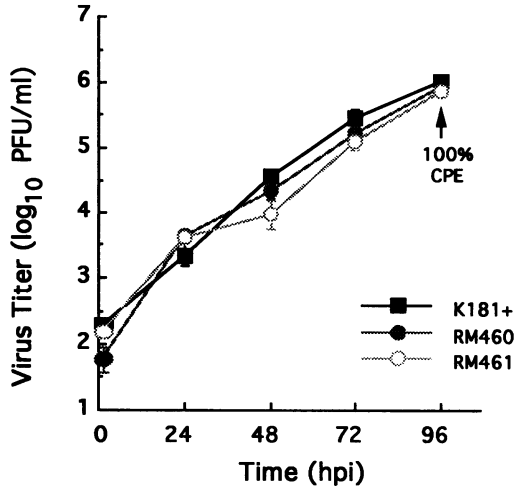

FIG. 5. Growth of wild-type murine CMV (K181$^+$), RM461, and RM460. Murine NIH 3T3 cells (10^5) were infected at an MOI of 0.1 PFU/ml, and, at the time points indicated, freeze-thaw supernatant was assayed for virus by plaque assay on NIH 3T3 cells. The standard deviation of the geometric mean of triplicate cultures was less than 0.5 (error bars). CPE, cytopathic effect.

duced a number of unexpected *ie2-lacZ* hybrid transcripts in the 7.2-kb range that were not observed at any time with RM461. It remains unclear whether these aberrant transcripts were translated, but, as a result of their presence, we focused our attention on RM461 rather than RM460 for most studies.

In contrast to RM461, the *lacZ* transcript expressed by RM427 showed characteristics of an abundant α gene that was not subjected to any shutoff during infection. Transcripts and protein continued to accumulate to very high levels throughout infection. Under cycloheximide block, expression from RM427 was even more abundant than from RM408, a virus with *lacZ* under the control of the murine CMV *ie*1 promoter-enhancer (33, 34), a result that may be attributed to the combined activity of the human CMV promoter-enhancer and the adjacent murine CMV enhancer in RM427. Furthermore, the characteristic shutoff of expression that occurred when *lacZ* expression was placed under the control of the murine CMV *ie*1/*ie*3 promoter-enhancer (34, 39, 47) did not take place when the human CMV enhancer was used. The accumulation of β-gal during infection was very similar to that in RM461 (Fig. 4), although higher, but, as with RM461, expression was severely reduced when infection was carried out in the presence of phosphonoformate (data not shown). Taken together with results on RM460 and RM461, it appeared that the same *lacZ* insert was subjected to differential temporal control depending on the nature of the promoter used, the particular insert site, and the orientation of the insert within the viral genome.

Growth and virulence characteristics of RM460 and RM461. After infection with an MOI of 0.1 PFU per cell, the rate of growth exhibited by recombinant viruses in cultured cells was identical to that of parental K181$^+$ virus, and both reached 100% cytopathic effect by 4 days p.i. (Fig. 5). We had previously found that RM427 also exhibited completely normal levels of growth in cultured cells (33, 35). The size and morphology of virus plaques were identical in recombinant and parental viruses, and stock titers for RM460, RM461, and wild-type K181$^+$ were all similar. Thus, recombinant viruses exhibited the same growth characteristics in cultured cells as did parental wild-type virus. These results also indicate that the γ0.85 gene, which is disrupted in RM460 and RM461, represents yet another murine CMV gene that is dispensable for growth in cultured fibroblast cells.

The recombinant viruses were compared with the parental wild type for virulence in 3-week-old BALB/c mice. Tissue culture-propagated virus stocks were used to perform i.p. inoculations of groups of four or five animals at 1×10^6, 3×10^6, and 1×10^7; following inoculation, these animals were evaluated twice daily. The LD_{50} data shown in Table 1 indicate that all recombinant viruses were as virulent for BALB/c mice as the parental wild-type strain K181$^+$ was. Thus, the γ0.85 gene represents a murine CMV gene that does not severely impact virulence for immunocompetent mice.

We evaluated RM461 viral growth in various organs of the mouse following i.p. inoculation of groups of five BALB/c mice with 10^4 PFU from salivary gland-propagated virus stocks. Tissue and blood samples were assayed for virus at 3, 5, 7, 9, 14, 21, 28, and 42 days p.i. As previously reported (4), titers of these viruses in the spleen, liver, adrenal glands, and lungs were all comparable to that of the parental wild type. For all tissues sampled, the growth of RM460 and RM461 was only markedly and consistently lower than that of the wild type in the salivary gland (Table 2), where it was generally 2 orders of

TABLE 1. Growth and virulence characteristics in BALB/c mice

Virus	LD_{50} (PFU)	Virus titer (PFU/g) at 3 days p.i.[a] in:		
		Spleen	Adrenals	Liver
K181$^+$	2×10^7	3×10^4	1×10^2	3×10^3
RM461	6×10^6	6×10^5	2×10^3	3×10^4
RM460	6×10^6	ND[b]	ND	ND
RM427	1×10^7	2×10^3	2×10^2	4×10^3

[a] Standard deviations of the geometric mean for all titers was <0.2 PFU/g.
[b] ND, not done.

TABLE 2. Peak virus titers in salivary gland of immunocompetent and immunodeficient mice

Virus	Virus titers (PFU/g) in:		
	BALB/c[a]	BALB/c (*nu/nu*)[a]	C.B17 (*scid/scid*)[b]
K181$^+$	3×10^8	4×10^7	3×10^8
RM461	1×10^6	3×10^4	4×10^4
RM427	2×10^2	ND[c]	2×10^2

[a] Titer at 13 to 14 days p.i.
[b] Titer at 21 days p.i.
[c] ND, not done.

magnitude below that of the wild type. This effect has been observed in other *lacZ*-positive viruses and appeared to be intrinsic, because the effect was not overcome by passing viruses through the animal. This defect was not the result of the γ0.85 gene disruption but was due to the presence and expression of the *lacZ* gene. Every *lacZ*-tagged murine CMV we have evaluated, regardless of insert site, has exhibited this organ-specific reduction in peak titers. Also relevant to this point is that all of our work characterizing the *sgg*1 gene (28, 35), a viral gene that affects growth in the salivary gland, and the *ie*2 gene (4), a gene with no apparent effect on the virus, has relied on comparisons of viral mutants that are controlled for the presence of a *lacZ* insert. We also investigated whether the reduced growth of *lacZ*-positive insertion mutants resulted from an immune response to β-gal by examining the growth properties of RM461 in nude (BALB/c *nu/nu*) or in SCID (C.B17 *scid/scid*) mice. As shown in Table 2, RM461 exhibited reduced growth patterns in salivary glands of immunodeficient mice, similar to the behavior in immunocompetent BALB/c mice. These data suggested that the presence of the insertion or expression of β-gal, and not simply an immune response to β-gal, caused the lower yields of virus in the salivary gland. Importantly, this significantly reduced level of growth was not observed in any tissues other than the salivary gland of either immunocompetent or immunodeficient mice, and therefore we went on to characterize more fully the interaction of RM461 with the host.

Latency characteristics of *lacZ*-tagged CMVs. The capacity for latent infection in the spleen of BALB/c mice and continued expression of *lacZ* during latency, a technique that we had successfully pioneered in the study of HSV-1 latency (14), were two characteristics that we had hoped to preserve in recombinant viruses. Latency established following i.p. inoculation can be readily demonstrated by explant culture. K181$^+$, RM461, RM460, and RM427 were all introduced into groups of 7 to 10 3-week-old BALB/c mice. At 4 months p.i., virus reactivation was sought by explant of spleen cells and the level of persistent virus was measured by culturing salivary gland homogenates directly on susceptible cultured cells. The recombinant viruses showed a full capacity for latent infection as measured by the presence of detectable virus in the supernatant of explanted spleen fragments (Fig. 6). RM461 was also reactivated as readily as was parental wild-type virus following immunosuppression with anti-CD4 and anti-CD8 monoclonal antibodies (4). Thus, these recombinant viruses retained characteristic latent-infection qualities. To our disappointment, when latently infected spleens and salivary glands (from RM461- or RM427-infected animals) were examined for continued expression of β-gal, they were found to be uniformly negative. Thus, *lacZ* expression was not constitutive in infected animals.

Localization of virus in leukocytes. The ability of *lacZ*-tagged recombinant CMV to associate with a particular blood

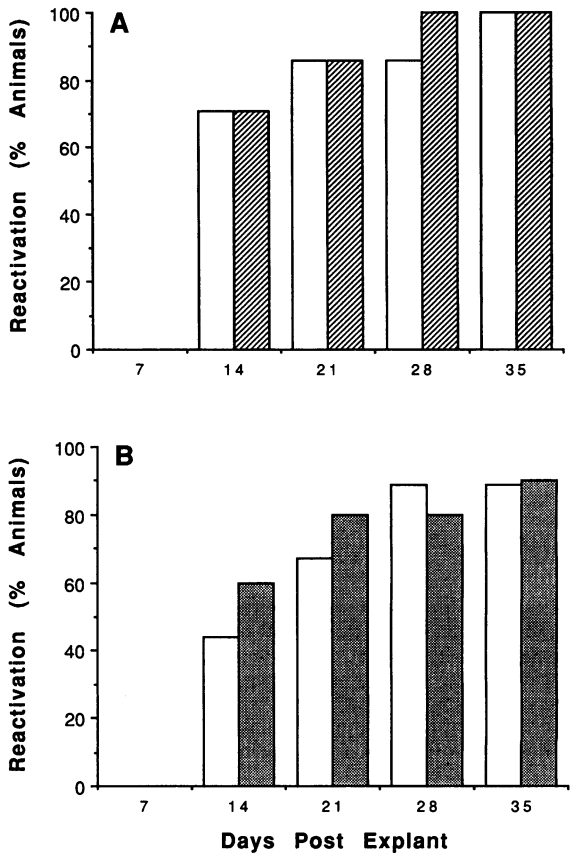

FIG. 6. Latency and reactivation of *lacZ*-tagged viruses. (A) Explant reactivation of RM461 (hatched bars) compared with K181$^+$ (open bars). At 16 weeks after i.p. inoculation with 10^5 PFU of salivary gland stock of virus, groups of eight infected BALB/c mice were sacrificed and spleen fragments were cultured. (B) Explant reactivation of RM427 (shaded bars) and K181$^+$ (open bars). At 16 weeks after i.p. inoculation with 10^6 PFU of cell culture stock of virus, groups of 9 (K181) or 10 (RM427) infected BALB/c mice were sacrificed and spleen fragments were cultured. At weekly intervals, the supernatant was plaque assayed for virus, and the percentage of total animals yielding virus up to 35 days postexplant is shown. Virus was not detected at 7 days postexplant in any animals.

cell population during acute infection was evaluated at 5 days after i.p. inoculation with 10^5 PFU of salivary gland-propagated virus. Although RM461 reached peak titers in blood by 5 days p.i., there were very few positive cells during this period. After lysis of erythrocytes, 10^6 leukocytes were initially cytocentrifuged onto glass slides, fixed in 0.5% glutaraldehyde, and stained with X-Gal, after which approximately 4 to 20 mononuclear cells were positive (data not shown). This level is in agreement with the very low level of viremia (virus-infected cells) that can be detected in infected immunocompetent animals (35). When leukocytes were allowed to attach to glass prior to analysis, the percentage of stained cells increased more than 100-fold. As many as 0.1% of attached cells stained blue after X-Gal overlay (Fig. 7A). These cells averaged 15 to 20 μm in diameter and thus were larger than most attached cells (Fig. 7B). These cells were specifically infected with the *lacZ*-tagged virus and did not represent background, because they were not detected in K181$^+$-infected mice. The glutaraldehyde fixation protocol we used here has previously been shown to inactivate lysosomal β-gal (13) that would otherwise result in staining of unfixed monocytes from uninfected ani-

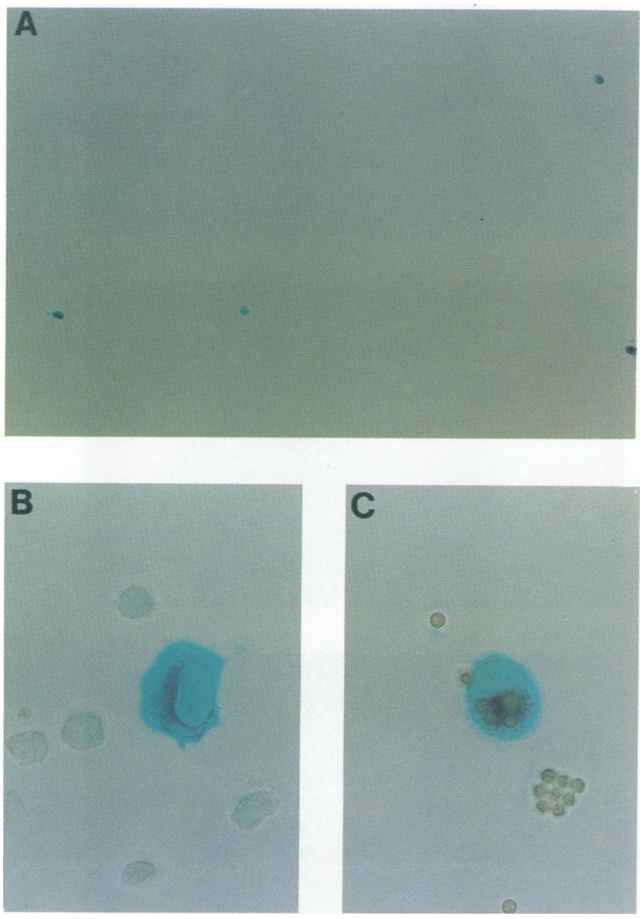

FIG. 7. Identification of infected cells in the peripheral blood. X-Gal-stained glass-adherent cells at 5 days after i.p. inoculation with RM461 are shown. (A) Glass-adherent cells (approximately 3,000 cells in the field) showing four blue-stained cells. Magnification, ×100. (B) Large (18 to 20 μm in diameter) stained mononuclear cell surrounded by smaller (10 μm) glass-adherent cells. Magnification, ×1,000. (C) Glass-adherent large stained cell with internalized 3-μm-diameter latex beads. A smaller nonstained phagocytic cell with eight beads is shown adjacent to the stained cell. Magnification, ×1,000.

mals. Furthermore, when plastic-adherent cells were disrupted by sonication and the resultant lysate was assayed on permissive NIH 3T3 cells, virus was recovered (data not shown).

X-Gal-positive, attached cells had a mononuclear cell morphology (Fig. 7B); therefore we sought to determine whether these cells exhibited phagocytic capability. Leukocytes were allowed to attach to glass for 4 h in the presence of 3-μm-diameter latex beads. Following fixation and staining with X-Gal, every blue-staining cell (over 100 were observed in several fields of cells from different animals) was found to have phagocytized at least 1 bead, and some had taken up as many as 10 beads. Thus, all X-Gal-stained, infected cells were found to be phagocytic, large mononuclear cells (Fig. 7C). We investigated whether these attached cells were monocytes by subjecting acetone-fixed cells to a two-color immunofluorescence analysis with rabbit antibody to major histocompatibility complex class II or rat monoclonal antibodies to MAC-1 α chain, along with a rabbit anti-β-gal antiserum to detect the cells infected with *lacZ*-tagged murine CMV. The β-gal-positive cells failed to react with either of these two monocyte markers, suggesting that this infected population of cells lacked typical monocyte surface markers (data not shown). Uninfected attached cells with these monocyte markers were readily detected adjacent to the infected cells on the same slides. These infected peripheral blood cells were mononuclear, capable of attaching to glass, and efficient at phagocytizing latex beads, suggesting that they exhibited the characteristics of the precursor of monocytes, dendritic cells and granulocytes (17), for which no specific cell surface markers currently exist. Whatever their true nature, they are large mononuclear cells that appear to be responsible for viral dissemination.

Localization of virus in organs. To assess the distribution of *lacZ*-tagged virus in tissues early in acute infection and to demonstrate that the behavior of recombinant viruses was consistent with more-conventional investigations with wild-type murine CMV, we monitored the course of virus from the inoculation site in the spleen, adrenal glands, liver, and salivary gland by staining frozen sections for the presence of β-gal-positive cells. After i.p. inoculation with either cell culture- or salivary gland-passaged stocks, cell-associated and cell-free viral progeny are first detected in the peritoneal cavity at 48 h p.i. (33), and the host cell supporting replication is believed to be a peritoneal macrophage (54). At 2 days p.i. with either 10^5 PFU of salivary gland-propagated RM461 stock or 10^6 PFU of tissue culture-propagated RM427 stock, when progeny viruses were being released at high levels, cells in the peritoneal cavity were stained intensely with X-Gal, even when viewed macroscopically (Fig. 8A). The cells that stained at this time were identified as mesothelial cells that lined all membranes exposed to this cavity, including the spleen capsule (Fig. 8B). Thus, virus was produced by cell types other than the expected site (macrophages) in the peritoneal cavity.

By 3 days after i.p. inoculation, virus can be readily detected at highest titers in the spleen, liver, and adrenal glands (4). After inoculation with RM461, foci of X-Gal-staining cells were clearly visible in the perifollicular areas of the spleen, throughout the liver, and in the cortex of the adrenal glands (Fig. 8C to F). With the better resolution available by using paraffin-embedded sections, the site of viral replication in the spleen is readily visualized as being associated with cells that line venules leading to lymphoid follicles. Although these cells were previously identified as factor VIII-positive endothelial cells (38), we found that few, if any, β-gal-positive cells stained positive with a factor VIII-specific antibody in a two-color immunofluorescence analysis (data not shown). The distribution of virus infection, shown here as previously (38, 42), follows the distribution of marginal-zone macrophages or dendritic cells in the spleen (27, 58). These data suggest that mononuclear phagocytes in blood may be the precursors of cells supporting viral replication in the spleen. Additional work is needed to resolve the relative contribution of macrophages, dendritic cells, and endothelial cells as sites of viral replication in the spleen.

At 3 days p.i., we also found virus replicating to high levels in brown fat (Fig. 8G), and this tissue had large focal areas of infection clearly evident at 6 days p.i. (Fig. 8H). The brown fat provided an excellent site to observe the inflammatory clearance of infected cells that occurs starting at about 7 days p.i. and is associated with the induction of a strong cellular immune response (26); by 9 days p.i., blue X-Gal-staining cells were no longer detectable at this site. In their place was an equivalent number of foci of inflammatory mononuclear cells (Fig. 8I). After the resolution of acute infection, neither viruses nor X-Gal-staining cells continued to be detected in any of these tissues.

The salivary gland did not have detectable stained foci at 3

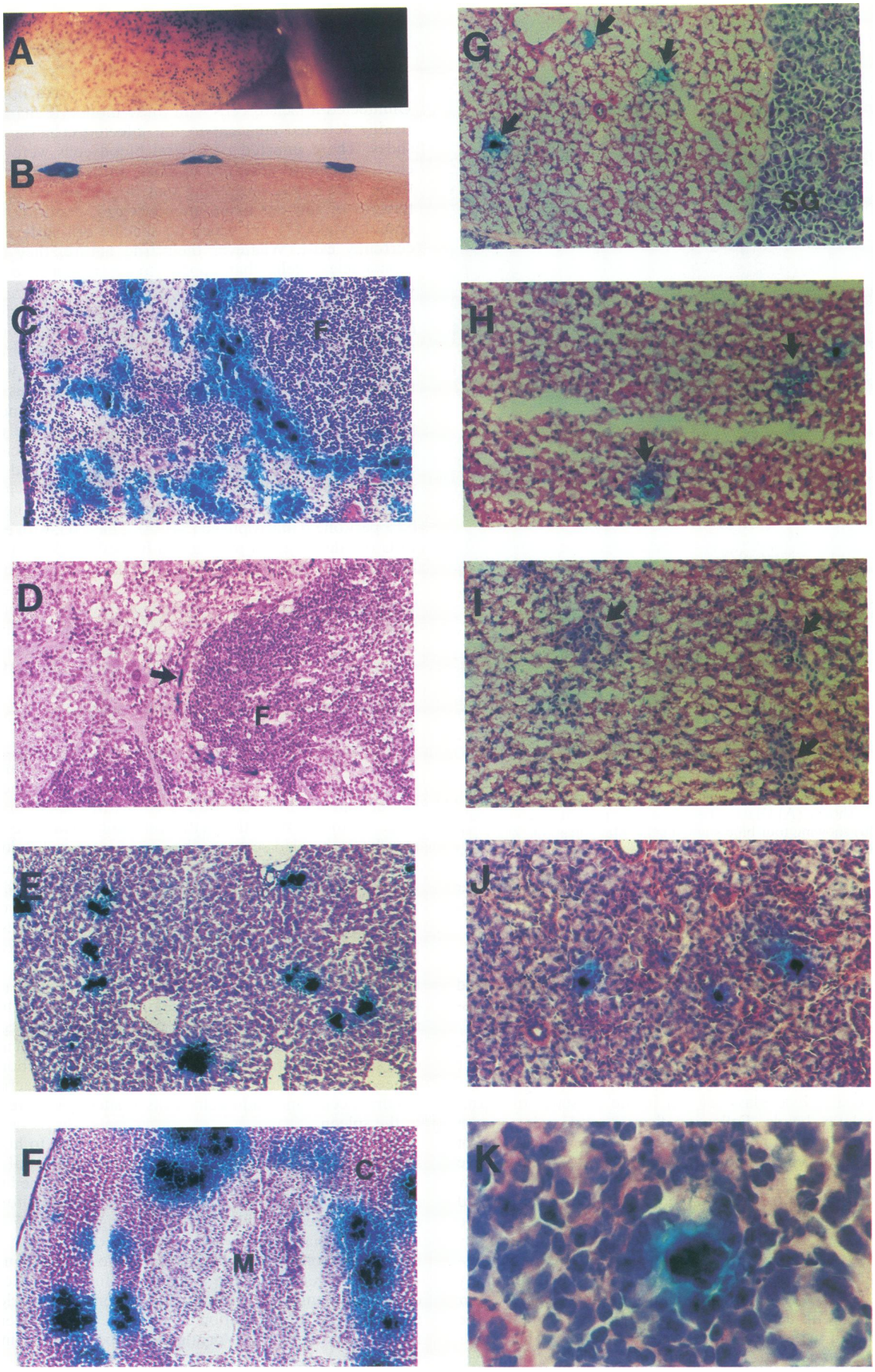
A
B
C
F
D
F
E
F
C
M
G
SG
H
I
J
K

days p.i. X-Gal-stained serous acinar cells were first observed at 6 days p.i. and reached maximal numbers and size by 9 days p.i. (Fig. 8J and K), a time when virus was being cleared from other tissues, including the brown fat immediately adjacent to the salivary gland (Fig. 8I). Infiltrating inflammatory cells were also present in the salivary gland at this time (Fig. 8J), although virus was not cleared from this organ for several additional weeks, a phenomenon which has been attributed to a cytokine-mediated process that is distinct from the cytotoxic T-cell response that clears virus from most tissues (20). This staining pattern continued at least through 21 days p.i. Even though RM461 did not replicate to titers as high as the parental strain $K181^+$ did, the cellular site of replication and distribution is similar to that established for wild-type murine CMV (36, 43).

DISCUSSION

We have constructed *lacZ*-tagged recombinant murine CMV strains and have used these viruses to track viral dissemination to the prominent organs that are involved in acute infection. Our results suggest that mononuclear phagocytes are the primary vehicle for viral dissemination from the i.p. site of inoculation but that they fail to show typical surface markers of monocytes, possibly as a result of viral infection or because they represent dendritic cell precursors (18, 19). Only a small percentage of phagocytic mononuclear cells appear to be actively supporting viral replication, as indicated by the small numbers of X-Gal-staining cells we observed here at 5 days p.i. This low level of stained cells agrees with the low-level, cell-associated viremia that has been documented by the recovery of virus from cultured leukocytes (2, 35). This work lends support to the different ways that CMV-mononuclear cell interaction has been viewed as critical to virus biology (8, 16, 29, 32, 50, 62). Our work suggests that these cells may deliver virus to the various tissues and organs during acute infection as it differentiates from its site of origin in the bone marrow. We suspect that blood cells initially become infected by virus released in the peritoneal cavity; however, peak levels in the blood are not reached until 4 to 5 days after i.p. inoculation, suggesting that this issue needs further evaluation.

In the design of RM427 and RM461, we chose the human CMV *ie1/ie2* promoter-enhancer to drive expression of *lacZ* because we observed that its expression was stronger than that of the natural murine CMV *ie1* promoter-enhancer when inserted at this site in the viral genome (22, 33, 34). We also predicted that continued expression of the indicator enzyme might occur during latency in the spleen as well as in other tissues. Despite its strong expression during acute replication, we have been unable to detect continued expression of β-gal in the latently infected spleen by using X-Gal or other β-gal substrates. We believe that the readily detectable immune response to β-gal (33) probably contributes to this shutdown of expression. Even though RM461 carried the same *lacZ* cassette as RM427, the site of insertion was farther from the murine CMV enhancer and the consequent expression of β-gal showed markedly different characteristics. Expression was barely detectable immediately after infection or in the presence of cycloheximide and tended to show kinetics and sensitivity to phosphonoformate more characteristic of a γ gene. In either RM461- or RM427-infected animals, the disappearance of X-Gal staining correlates with the disappearance of infectious virus from tissues, and we therefore believe that the stained cells identified here are all actively supporting viral replication. Consistent with the notion that X-Gal-stained cells undergo productive replication, the level of expression of β-gal in RM461-infected cells was highest at late times in infection. In immunodeficient SCID mice, in which viral replication is never brought under control and animals succumb to as little as 10 PFU of wild-type CMV, β-gal continues to be readily detected and to accumulate in various tissues.

The large monocytic phagocytes that were observed in the peripheral blood lacked the typical antigens associated with monocytes. These antigens were readily detected on uninfected, smaller, glass-adherent cells present in the same cultures with the larger, infected cells. On the one hand, the large size of these cells and their lack of typical monocyte markers could be due to effects of virus, although typical cytomegaly and inclusions were not observed. CMV is known to alter the expression of cell surface markers, possibly leading to down-regulation of major histocompatibility complex class II and MAC-1α antigens. On the other hand, the large size of these cells, the phagocytic properties, the lack of major histocompatibility complex class II expression, and the small numbers are consistent with these cells being dendritic cell precursors (18, 19). This issue can be resolved only through further investigations with additional cell-typing reagents.

Virus-infected cells in spleens were localized primarily in the perifollicular region between the red and white pulp, consistent with previous reports (38, 42). In contrast to the conclusion drawn in the most recent study (38), however, we found little overlap between the infected-cell population and factor VIII-positive cells by two-color immunofluorescence analysis. Thus, on the basis of the staining pattern, these cells may be either marginal-zone macrophages or dendritic cells that localize to the venules as they traffic out of the peripheral blood.

Staining in other organs of recombinant virus-infected mice was largely consistent with previous results obtained with wild-type viruses (36, 43). The most intensely infected organs early after inoculation were the spleen, liver and adrenal glands. In adrenal glands, replication was localized to the cortex, consistent with the previously reported behavior in older mice (43). The cortical region is responsible for glucocorticoid production, and CMV infection may disrupt this process, even though animals that survive infection have shown no long-term damage. In the liver, replication was multifocal and has recently been associated with the mortality that can occur

FIG. 8. Identification of infected X-Gal-stained cells in the peritoneal cavity, spleen, liver, adrenal gland, brown fat, and salivary gland. (A) Peritoneal cavity of an animal at 2 days p.i. with RM427 exposed and stained with X-Gal. Magnification, ×10. (B) Frozen section (10 μm) of spleen showing X-Gal staining of mesothelial cells. Magnification, ×300. (C) Frozen section (10 μm) of spleen at 3 days p.i. with RM461 showing perifollicular X-Gal staining. Magnification, ×150. (D) Paraffin-embedded section (3 μm) at 3 days p.i. with RM427 showing perifollicular staining. Magnification, ×400. (E) Frozen section (10 μm) of liver at 3 days p.i. with RM461 showing scattered X-Gal-stained foci. Magnification, ×100. (F) Frozen section (10 μm) of adrenal gland at 3 days p.i. with RM461 showing large foci of X-Gal-stained cells in the cortex. Magnification, ×100. (G) Frozen section (10 μm) of brown fat and adjacent salivary gland at 3 days p.i. with RM461 showing early X-Gal-stained foci of infection in brown fat. Magnification, ×200. (H) Frozen section (10 μm) of brown fat at 6 days p.i. with RM461 showing three well-developed X-Gal-stained foci of infection. Magnification, ×200. (I) Frozen section (10 μm) of brown fat at 9 days p.i. with RM461 showing an inflammatory cell infiltrate. Magnification, ×200. (J) Frozen section (10 μm) of submaxillary salivary gland at 9 days p.i. with RM461 showing X-Gal-stained foci. Magnification, ×200. (K) Frozen section (10 μm) of submaxillary salivary gland at 9 days p.i. with RM461 showing X-Gal-stained serous acinar cells. Magnification, ×1,000. Samples C to K were all stained with hematoxylin and eosin in addition to X-Gal.

in immunocompetent mice (52). Infection of the brown fat paralleled infection in these organs, being detectable initially at 3 days p.i.; replacement of the lesions resulting from virus replication with mononuclear infiltrates took place between 6 and 9 days p.i.

We first observed virus appearing in the salivary gland between 3 and 6 days p.i.; however, peak titers of *lacZ*-tagged recombinant viruses were reduced in this organ. This reduction in peak titers did not appear to result from a disruption of a particular murine CMV gene, from any changes in normal tropism, or from rapid clearance due to the immune response; rather, it appeared to be due to the expression of β-gal. Both nude and SCID mice exhibited organ-specific reductions as well. We do not understand why the presence of the insert would result in a phenotype of reduced growth in salivary gland, but the virus still targeted serous acinar epithelial cells. Importantly, RM461 exhibited normal growth properties in cultured cells as well as in other tissues such as the spleen, liver, adrenal glands, and lungs of the experimentally infected BALB/c mouse (4), was fully virulent, and was fully capable of latency. Despite differences in peak titers in the salivary gland, the target cell remained the same. This study establishes the value of *lacZ*-tagged viruses for studies of viral tropism, pathogenesis, or latency.

We found that the mesothelial cells lining the peritoneal cavity were efficiently infected. These mesothelial cells are likely to contribute significantly to the cell-free virus that can be detected in the peritoneal cavity within 48 h p.i. Previous focus on the macrophage as the most likely cell type harboring virus in the peritoneal cavity resulted in many reports that differed in the extent to which this population of cells could be shown to be permissive (3, 21, 41, 54, 63). We found that the mesothelial cells efficiently supported viral infection whether the virus stock used for inoculation was derived from the salivary gland or from cultured fibroblast cells. Thus, differences in the preparation of virus stocks did not have any dramatic impact on the growth we observed in the peritoneal cavity.

The mouse remains a very appropriate host for studying many aspects of CMV biology. We have presented results that suggest that *lacZ*-tagged murine CMV makes tropism studies in this host much more approachable, a strategy that was found to work well for herpes simplex virus (13, 14). The viruses and methods described here can be used to investigate a range of issues in virus biology, and when combined with methods for rapid generation of recombinant viruses (34, 65), this approach can be used to investigate the function of the large number of viral genes expected to play subtle roles in the biology of this virus infection.

ACKNOWLEDGMENTS

We thank M. Kirichenko for preparation of cells and virus stocks; Y.-C. Lin for the MUG assays on RM461 and RM427; J. Vieira for original detection of the γ0.85 transcript; and G. Shellam, T. Scalzo, and N. Fitzgerald for titer determinations in BALB/c (*nu/nu*) mice.

This work was supported by PHS research grants RO1 AI30363 and RO1 AI28341. C.A.S., R.D.C., and W.C.M. were supported by PHS training grant T32 AI07328, and R.D.C. was supported by PHS grant NSRA 5F32 AI08420.

REFERENCES

1. **Alford, C. A., and W. J. Britt.** 1993. Cytomegalovirus, p. 227–255. *In* B. Roizman, R. J. Whitley, and C. Lopez (ed.), The human herpesviruses. Raven Press, New York.
2. **Bale, J. F., Jr., and M. E. O'Neil.** 1989. Detection of murine cytomegalovirus DNA in circulating leukocytes harvested during acute infection of mice. J. Virol. **63**:2667–2673.
3. **Brautigam, A. R., F. J. Dutko, L. B. Olding, and M. B. Oldstone.** 1979. Pathogenesis of murine cytomegalovirus infection: the macrophage as a permissive cell for cytomegalovirus infection, replication and latency. J. Gen. Virol. **44**:349–359.
4. **Cardin, R. D., J. M. Boname, G. B. Abenes, S. A. Jennings, and E. S. Mocarski.** 1993. Reactivation of murine cytomegalovirus from latency, p. 101–110. *In* S. Plotkin and S. Michelson (ed.), Multidisciplinary approaches to understanding cytomegalovirus disease. Elsevier Biomedical Press, Amsterdam.
5. **Cherrington, J. M., and E. S. Mocarski.** 1989. Human cytomegalovirus ie1 transactivates the α promoter-enhancer via an 18-base-pair repeat element. J. Virol. **63**:1435–1440.
6. **Cheung, K. S., and D. J. Lang.** 1977. Transmission and activation of cytomegalovirus with blood transfusion: a mouse model. J. Infect. Dis. **135**:841–845.
7. **Dankner, W. M., J. A. McCutchan, D. D. Richman, K. Hirata, and S. A. Spector.** 1990. Localization of human cytomegalovirus in peripheral blood leukocytes by in situ hybridization. J. Infect. Dis. **161**:31–36.
8. **Dudding, L. R., and H. M. Garnett.** 1987. Interaction of strain AD169 and a clinical isolate of cytomegalovirus with peripheral monocytes: the effect of lipopolysaccharide stimulation. J. Infect. Dis. **155**:891–896.
9. **Feinberg, A. P., and B. Vogelstein.** 1984. A technique for radiolabeling DNA restriction endonuclease fragments to high specific activity. Anal. Biochem. **137**:266–267.
10. **Geballe, A. P., F. S. Leach, and E. S. Mocarski.** 1986. Regulation of cytomegalovirus late gene expression: γ genes are controlled by posttranscriptional events. J. Virol. **57**:864–874.
11. **Geballe, A. P., R. R. Spaete, and E. S. Mocarski.** 1986. A cis-acting element within the 5′ leader of a cytomegalovirus β transcript determines kinetic class. Cell **46**:865–872.
12. **Grefte, A., M. van der Giessen, W. van Son, and T. H. The.** 1993. Circulating cytomegalovirus (CMV)-infected endothelial cells in patients with an active CMV infection. J. Infect. Dis. **167**:270–277.
13. **Ho, D. Y., and E. S. Mocarski.** 1988. β-Galactosidase as a marker in the peripheral and neural tissues of the herpes simplex virus-infected mouse. Virology **167**:279–283.
14. **Ho, D. Y., and E. S. Mocarski.** 1989. Herpes simplex virus latent RNA (LAT) is not required for latent infection in the mouse. Proc. Natl. Acad. Sci. USA **86**:7596–7600.
15. **Ho, M.** 1980. Role of specific cytotoxic lymphocytes in cellular immunity against murine cytomegalovirus. Infect. Immun. **28**:49–53.
16. **Ibanez, C. E., R. Schrier, P. Ghazal, C. Wiley, and J. A. Nelson.** 1991. Human cytomegalovirus productively infects primary differentiated macrophages. J. Virol. **65**:6581–6588.
17. **Inaba, K., M. Inaba, M. Deguchi, K. Hagi, R. Yasumizu, S. Ikehara, S. Muramatsu, and R. M. Steinman.** 1993. Granulocytes, macrophages, and dendritic cells arise from a common major histocompatibility complex class II-negative progenitor in mouse bone marrow. Proc. Natl. Acad. Sci. USA **90**:3038–3042.
18. **Inaba, K., M. Inaba, M. Naito, and R. M. Steinman.** 1993. Dendritic cell progenitors phagocytose particulates, including bacillus Calmette-Guerin organisms, and sensitize mice to mycobacterial antigens in vivo. J. Exp. Med. **178**:479–488.
19. **Inaba, K., R. M. Steinman, M. W. Pack, H. Aya, M. Inaba, T. Sudo, S. Wolpe, and G. Schuler.** 1992. Identification of proliferating dendritic cell precursors in mouse blood. J. Exp. Med. **175**:1157–1167.
20. **Jonjic, S., W. Mutter, F. Weiland, M. J. Reddehase, and U. H. Koszinowski.** 1989. Site-restricted persistent cytomegalovirus infection after selective long-term depletion of $CD4^+$ T lymphocytes. J. Exp. Med. **169**:1199–1212.
21. **Jordan, M. C., and V. L. Mar.** 1982. Spontaneous activation of latent cytomegalovirus from murine spleen explants. Role of lymphocytes and macrophages in release and replication of virus. J. Clin. Invest. **70**:762–768.
22. **Keil, G. M., K. A. Ebeling, and U. H. Koszinowski.** 1984. Temporal regulation of murine cytomegalovirus transcription and mapping of viral RNA synthesized at immediate early times after infection.

J. Virol. **50**:784–795.
23. **Keil, G. M., K. A. Ebeling, and U. H. Koszinowski.** 1987. Immediate-early genes of murine cytomegalovirus: location, transcripts, and translation products. J. Virol. **61**:526–533.
24. **Keil, G. M., K. A. Ebeling, and U. H. Koszinowski.** 1987. Sequence and structural organization of murine cytomegalovirus immediate-early gene 1. J. Virol. **61**:1901–1908.
25. **Klotman, M. E., S. C. Henry, R. C. Greene, P. C. Brazy, P. E. Klotman, and J. D. Hamilton.** 1990. Detection of mouse cytomegalovirus nucleic acid in latently infected mice by in vitro enzymatic amplification. J. Infect. Dis. **161**:220–225.
26. **Koszinowski, U. H., M. del Val, and M. J. Reddehase.** 1990. Cellular and molecular basis of the protective immune response to cytomegalovirus infection. Curr. Top. Microbiol. Immunol. **154**: 189–220.
27. **Kraal, G.** 1992. Cells in the marginal zone of the spleen. Int. Rev. Cytol. **132**:31–74.
28. **Lagenaur, L. A., J. Vieira, C. L. Martens, and E. S. Mocarski.** The structure and function of the murine cytomegalovirus *sgg*1 gene: a determinant of viral growth in salivary gland acinar cells. Submitted for publication.
29. **Lathey, J. L., and S. A. Spector.** 1991. Unrestricted replication of human cytomegalovirus in hydrocortisone-treated macrophages. J. Virol. **65**:6371–6375.
30. **Leach, F. S., and E. S. Mocarski.** 1989. Regulation of cytomegalovirus late-gene expression: differential use of three start sites in the transcriptional activation of ICP36 gene expression. J. Virol. **63**:1783–1791.
31. **Lucin, P., I. Pavic, B. Polic, S. Jonjic, and U. H. Koszinowski.** 1992. Gamma interferon-dependent clearance of cytomegalovirus infection in salivary glands. J. Virol. **66**:1977–1984.
32. **Maciejewski, J. P., E. E. Bruening, R. E. Donahue, S. E. Sellers, C. Carter, N. S. Young, and S. St. Jeor.** 1993. Infection of mononucleated phagocytes with human cytomegalovirus. Virology **195**: 327–336.
33. **Manning, W. C.** 1990. Ph.D. thesis. Stanford University, Stanford, Calif.
34. **Manning, W. C., and E. S. Mocarski.** 1988. Insertional mutagenesis of the murine cytomegalovirus genome: one prominent alpha gene (ie2) is dispensable for growth. Virology **167**:477–484.
35. **Manning, W. C., C. A. Stoddart, L. A. Lagenaur, G. B. Abenes, and E. S. Mocarski.** 1992. Cytomegalovirus determinant of replication in salivary glands. J. Virol. **66**:3794–3802.
36. **McCordock, H. A., and M. G. Smith.** 1936. The visceral lesions produced in mice by salivary gland virus of mice. J. Exp. Med. **63**:303–310.
37. **Mercer, J. A., J. R. Marks, and D. H. Spector.** 1983. Molecular cloning and restriction endonuclease mapping of the murine cytomegalovirus genome (Smith strain). Virology **129**:94–106.
38. **Mercer, J. A., C. A. Wiley, and D. H. Spector.** 1988. Pathogenesis of murine cytomegalovirus infection: identification of infected cells in the spleen during acute and latent infections. J. Virol. **62**: 987–997.
39. **Messerle, M., B. Buhler, G. M. Keil, and U. H. Koszinowski.** 1992. Structural organization, expression, and functional characterization of the murine cytomegalovirus immediate-early gene 3. J. Virol. **66**:27–36.
40. **Messerle, M., G. M. Keil, and U. H. Koszinowski.** 1991. Structure and expression of murine cytomegalovirus immediate-early gene 2. J. Virol. **65**:1638–1643.
41. **Mims, C. A., and J. Gould.** 1978. The role of macrophages in mice infected with murine cytomegalovirus. J. Gen. Virol. **41**:143–153.
42. **Mims, C. A., and J. Gould.** 1978. Splenic necrosis in mice infected with cytomegalovirus. J. Infect. Dis. **137**:587–591.
43. **Mims, C. A., and J. Gould.** 1979. Infection of salivary glands, kidneys, adrenals, ovaries and epithelia by murine cytomegalovirus. J. Med. Microbiol. **12**:113–122.
44. **Mocarski, E. S.** 1993. Cytomegalovirus biology and replication, p. 173–226. *In* B. Roizman, R. Whitley, and C. Lopez (ed.), The human herpesviruses. Raven Press, New York.
45. **Mocarski, E. S., M. Bonyhadi, S. Salimi, J. M. McCune, and H. Kaneshima.** 1993. Human cytomegalovirus in a SCID-hu mouse: thymic epithelial cells are prominent targets of viral replication. Proc. Natl. Acad. Sci. USA **90**:104–108.
46. **Myerson, D., R. C. Hackman, J. A. Nelson, D. C. Ward, and J. K. McDougall.** 1984. Widespread presence of histologically occult cytomegalovirus. Hum. Pathol. **15**:430–439.
47. **Reddehase, M. J., M. R. Fibi, G. M. Keil, and U. H. Koszinowski.** 1986. Late-phase expression of a murine cytomegalovirus immediate-early antigen recognized by cytolytic T lymphocytes. J. Virol. **60**:1125–1129.
48. **Reddehase, M. J., W. Mutter, K. Munch, H. J. Buhring, and U. H. Koszinowski.** 1987. CD8-positive T lymphocytes specific for murine cytomegalovirus immediate-early antigens mediate protective immunity. J. Virol. **61**:3102–3108.
49. **Reddehase, M. J., F. Weiland, K. Munch, S. Jonjic, A. Luske, and U. H. Koszinowski.** 1985. Interstitial murine cytomegalovirus pneumonia after irradiation: characterization of cells that limit viral replication during established infection of the lungs. J. Virol. **55**:264–273.
50. **Rice, G. P., R. D. Schrier, and M. B. Oldstone.** 1984. Cytomegalovirus infects human lymphocytes and monocytes: virus expression is restricted to immediate-early gene products. Proc. Natl. Acad. Sci. USA **81**:6134–6138.
51. **Saltzman, R. L., M. R. Quirk, and M. C. Jordan.** 1988. Disseminated cytomegalovirus infection. Molecular analysis of virus and leukocyte interactions in viremia. J. Clin. Invest. **81**:75–81.
52. **Shanley, J. D., L. Biczak, and S. J. Forman.** 1993. Acute murine cytomegalovirus infection induces lethal hepatitis. J. Infect. Dis. **167**:264–269.
53. **Shanley, J. D., M. C. Jordan, and J. G. Stevens.** 1981. Modification by adoptive humoral immunity of murine cytomegalovirus infection. J. Infect. Dis. **143**:231–237.
54. **Shanley, J. D., and E. L. Pesanti.** 1983. Murine peritoneal macrophages support murine cytomegalovirus replication. Infect. Immun. **41**:1226–1233.
55. **Shanley, J. D., and E. L. Pesanti.** 1985. The relation of viral replication to interstitial pneumonitis in murine cytomegalovirus lung infection. J. Infect. Dis. **151**:454–458.
56. **Spaete, R. R., and E. S. Mocarski.** 1985. Regulation of cytomegalovirus gene expression: α and β promoters are *trans* activated by viral functions in permissive human fibroblasts. J. Virol. **56**:135–143.
57. **Spaete, R. R., and E. S. Mocarski.** 1987. Insertion and deletion mutagenesis of the human cytomegalovirus genome. Proc. Natl. Acad. Sci. USA **84**:7213–7217.
58. **Steinman, R. M.** 1991. The dendritic cell system and its role in immunogenicity. Annu. Rev. Immunol. **9**:271–296.
59. **Stevens, J. G., and M. L. Cook.** 1973. Latent infections induced by herpes simplex viruses. Cancer Res. **33**:1399–1401.
60. **Stoddart, C. A., and F. W. Scott.** 1988. Isolation and identification of feline peritoneal macrophages for in vitro studies of coronavirus-macrophage interactions. J. Leukocyte Biol. **44**:319–328.
61. **Taylor-Wiedeman, J., G. P. Hayhurst, J. G. Sissons, and J. H. Sinclair.** 1993. Polymorphonuclear cells are not sites of persistence of human cytomegalovirus in healthy individuals. J. Gen. Virol. **74**:265–268.
62. **Taylor-Wiedeman, J., J. G. Sissons, L. K. Borysiewicz, and J. H. Sinclair.** 1991. Monocytes are a major site of persistence of human cytomegalovirus in peripheral blood mononuclear cells. J. Gen. Virol. **72**:2059–2064.
63. **Tegtmeyer, P. J., and J. E. Craighead.** 1968. Infection of adult mouse macrophages in vitro with cytomegalovirus. Proc. Soc. Exp. Biol. Med. **129**:690–694.
64. **Turtinen, L. W., R. Salzman, M. C. Jordan, and A. T. Haase.** 1987. Interactions of human cytomegalovirus with leukocytes in vivo: analysis by in situ hybridization. Microb. Pathog. **3**:287–297.
65. **Vieira, J., H. E. Farrell, W. D. Rawlinson, and E. S. Mocarski.** 1994. Genes in the *Hin*dIII J fragment of the murine cytomegalovirus genome are dispensable for growth in cultured cells: insertion mutagenesis with a *lacZ/gpt* cassette. J. Virol. **68**:4837–4846.
66. **Winston, D. J., W. G. Ho, C. L. Howell, M. J. Miller, R. Mickey, W. J. Martin, C. H. Lin, and R. P. Gale.** 1980. Cytomegalovirus infections associated with leukocyte transfusions. Ann. Intern. Med. **93**:671–675.